



Energy flow analysis based on a simulated drive of a hybrid locomotive powered by fuel cells

Ireneusz Pielecha^{a,*} , Radostin Dimitrov^b , Veselin Mihaylov^c 

^a Institute of Combustion Engines and Powertrains, Poznan University of Technology, Poznan, Poland

^b Dept. Transport Engineering and Technologies, Technical University of Varna, Varna, Bulgaria

ARTICLE INFO

Received: 25 July 2022
 Revised: 8 August 2022
 Accepted: 9 August 2022
 Available online: 9 August 2022

KEYWORDS

rail vehicles
 energy flow
 hybrid vehicles
 fuel cell simulation
 high voltage battery

Implementation of hybrid drives in rail vehicles is a solution aimed at limiting the negative environmental impact of transport. The use of fuel cell systems is a contemporary trend in the development of locomotives. The paper presents an energy flow analysis in a hybrid locomotive powered using fuel cells. The parallel hybrid drive system consisted of fuel cells, batteries and an electric motor. The simulations and analyzes were performed with the use of AVL Cruise M software. A simulated route, with a length of approximately 300 km, was used as basis for the analysis, taking into account a typical speed profile of a locomotive in passenger traffic. The energy flow and consumption values were estimated, and mean hydrogen consumption values were determined.

This is an open access article under the CC BY license (<http://creativecommons.org/licenses/by/4.0/>)

1. Introduction

The number of locomotives powered by electricity has increased in recent years. In 2019, diesel was used as the main source of propulsion for locomotives only in Estonia, Latvia and Lithuania [10]. Electricity was the main source of power supply for traction vehicles (except locomotives) in Spain (87.4%), France (78.7%), Latvia (76%), Austria (72.9%), Poland (87.7%), Portugal (78.6%) and Sweden (96.8%) [10].

The densest rail networks in the EU in 2019 could be found in regions of Germany and the Czech Republic such as: Berlin (698 km/1000 km²) and Prague (491 km/1000 km²). High rail network densities (of about 120 km/1000 km²) were also recorded in other regions of the Czech Republic, Germany, the Netherlands and Poland – Fig. 1.

Implementing hybrid drives for use in rail vehicles is a trend that allows the reduction of the negative environmental impact of the transport sector. The share of hybrid drives in rail vehicles rose to approximately 4,900 units in 2020 and a further increase to 8,400 units is expected to take place by 2030 (this is an annual increase of approximately 5.5%) [13, 16].

Some companies, including: Alstom, Bombardier, Siemens, Wabtec Corporation and others, are investing in the development of trains powered by alternative fuels. Alstom was one of the first companies to present a locomotive with PEM (Proton Exchange Membrane) fuel cells powered by hydrogen fuel [4]. The hybrid battery-hydrogen system was equipped with fuel cells with a capacity of 400 kW and batteries with a capacity of 111 kW and an operational voltage of 800 V. Each of the traction motors had a power of 314 kW. Hydrogen was stored in special tanks with a hydrogen mass capacity of 2 × 94 kg at a pressure of 35 MPa [20]. In March 2018, Alstom received two orders for a total of 25 Coradia Lint hydrogen regional trains in southern Germany. As of today, these trains operate among others in: Italy, France, the Netherlands, Sweden and Austria [5]. In September 2018, Bombardier launched their own new Electro-Hybrid Train called Talent 3 [17].

The Japanese proposal for a hybrid drive rail solution with fuel cells was the HYBARI project, which was the result of cooperation between Toyota, Hitachi and the Japanese railways (JR East – East Japan Railway Company) [14, 15]. The vehicle uses two electric motors with a power of 95 kW each and a stack of

PEM fuel cells (four cells with a power of 60 kW) forming a Toyota Mirai module, and are supplemented by two Li-Ion batteries with an energy storage capacity of 2×120 kWh.

In Poland, the Corantia iLint locomotive was first presented in 2021 [8]. It is assumed that replacing one regional diesel train with a hydrogen train would result in the equivalent of retiring 400 cars from regular traffic on the roads [5].

Siemens offers the Mireo Plus H vehicle which runs on a battery-hydrogen drive. The system uses 200 kW fuel cells from Ballard. The vehicle range is estimated to be 600 km (for the two-unit system) and 1000 km (for the three-unit system) [22].

There are currently several projects for the use of fuel cells in various forms of transport:

1. IMMORTAL (IMproved lifetiMe stacks fOR heavy-duty Trucks through ultra-durabLe components); a project focusing on the development of fuel cells and their applications in heavy-duty vehicles
2. Flagships; a project to build a cargo ship powered by fuel cells
3. FCH2RAIL (Fuel Cell Hybrid Power Pack for Rail Applications); a project in which Belgium, Germany, Spain, Portugal and Toyota (as a supplier of fuel cells) participate to develop a zero-emission locomotive propulsion system
4. H2Haul (Hydrogen fuel cell trucks for heavy-duty, zero-emission logistics); testing of 16 heavy-duty vehicles equipped with fuel cells.

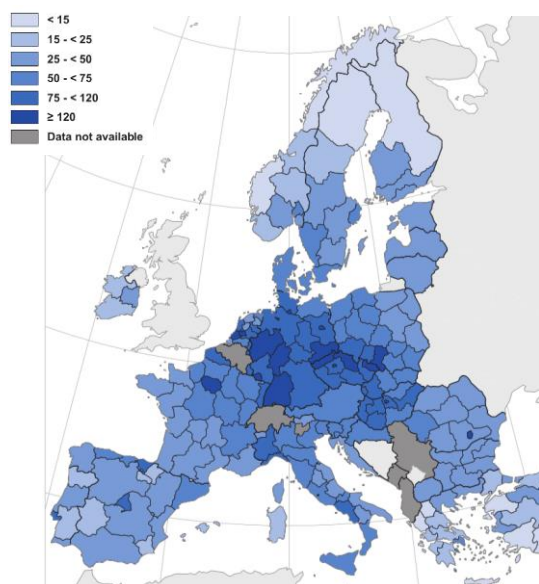


Fig. 1. European railway lines density in 2019 (in km of railway line per 1000 km²) [10]

2. Fuel cells in rail vehicles

Using fuel cell systems to power locomotives is a fairly modern trend in their development. Low-

temperature fuel cells are the ones most often used in transport means as a power source for electric motors [19]. In fuel cell (FC) systems, batteries are a necessary systems used for powering the fuel cells (in the first phase of their operation) and to generate supplementary power when driving in dynamic conditions, along with supercondensator (SC) due to their much higher power density values compared to batteries (BAT) [7, 11]. Research with the use of SC + BAT + FC conducted for vehicles of various classes (tram, passenger train, light rail vehicle, locomotive – tram, passenger train, railcar and freight locomotive) allowed for the optimal selection of power sources and energy storage [11, 12].

Simulation tests of hybrid rail vehicle systems with fuel cells can prove to be a significant source of information about the energy flow. Such studies enable the assessment of energy and hydrogen consumption in a locomotive traveling on a simulated route [1]. The simulation model presented in [1] included five modules: batteries, fuel cells, vehicle dynamics, power distribution and a controller. SOFCs (solid oxide fuel cells) require much higher temperature values to ensure their proper operation (to enable the flow of ions through the electrolyte). One of the proposals is a SOFC system with a Brayton turbine and a Rankin cycle [3]. Such a solution has made it possible to obtain an overall system efficiency of about 80%, while the efficiency of the cell itself was between just 45% and 65% [23]. The constant pressure to reduce the consumption of energy and fuel (including hydrogen) leads to optimization works in the field of eco-driving of such drives [6, 18], and the potential use of ammonia to power SOFC cells [2].

3. Aim of research work

The aim of the conducted research was to analyze the energy flow in the hybrid drive system of a locomotive equipped with fuel cells and high-voltage batteries. The analysis was performed on a typical route simulating traffic at speeds of up to 130 km/h. Energy consumption by drive systems and hydrogen consumption were all determined. The presented model enables the analysis and evaluation of hydrogen consumption on typical routes serviced currently by diesel locomotives.

4. Research method

4.1. Drive system model

The simulation test drives were carried out with the use of AVL Cruise M software. This software enables the simulation of energy flow processes in propulsion systems, including hybrid drives.

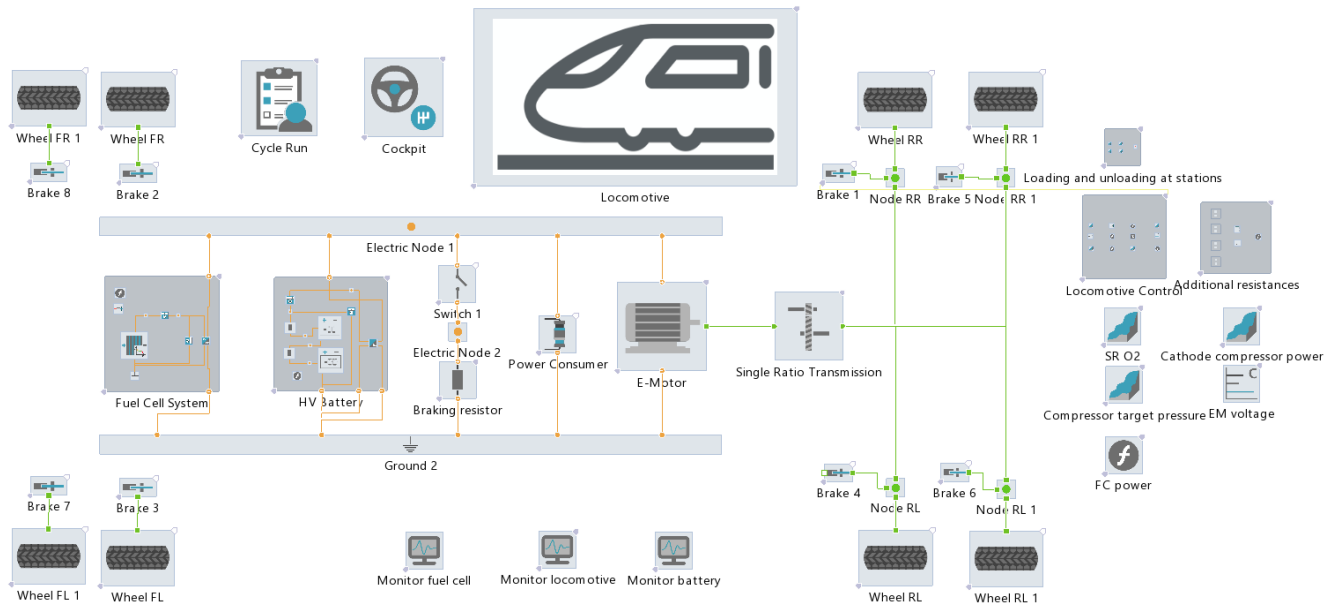


Fig. 2. Locomotive drive system model

The article presents an energy flow simulation in a locomotive (without carriages) that was equipped with fuel cells, batteries and an electric motor (Fig. 2). Some of the data included in the model was based on other papers [9, 21].

The locomotive, weighing 80 tons (Table 1), was equipped with an electric motor with a power of 2,600 kW. As shown in Fig. 2, the torque is transferred from the drive to the two axles. A low-temperature fuel cell system with a capacity of over 3 MW was connected in parallel to two batteries (connected in series) with a capacity of 1.7 MW as well as two DC-DC voltage converters. The fuel cell operated at a voltage of 4000–5000 V, the battery at about 2000 V and the electric motor at about 2000 V. Additionally, a braking resistor (power consumer) was included in the

system. It was activated when the braking power was greater than a specified maximum regenerative power. The locomotive had a wheelbase of 16 m and was equipped with a permanent gear with a ratio of 5.5 between the electric motor and the wheels. The function of resistance to motion is described by:

$$F = A + B \times V^2 \quad (1)$$

where: $a = 143 \text{ N}$, $b = 03399 \text{ N}/(\text{km}/\text{h})^2$, V – driving speed in km/h.

4.2. Scope of research

The energy flow tests were carried out on a regular locomotive route with a travel distance of 328 km. The simulation runtime was 14,225 s. The tests were carried out taking into account the locomotive mass of 82 t. The analysis covered the operating conditions of the fuel cell, the high-voltage battery and the electric motor. An analysis of energy flow, energy recuperation, and average energy consumption per 100 km was carried out.

5. Hybrid drive system with fuel cells

5.1. Fuel cells operating conditions

In the simulation model, 4,500 individual fuel cells with a total cell area of 2,720 cm² were used. The technical parameters of the fuel cell model were included in Table 2.

Because it is necessary to adjust the voltage value of the cells stack and the electric motor, the stack of fuel cells was connected to a DC-DC voltage converter (at 95% efficiency) (Fig. 3).

Table 1. Technical data of locomotive

Locomotive		
Distance from hitch to front axle	m	16
Wheel base	m	12
Height of support point at bench test	m	0.5
Distance from point of force application to front axle	mm	4000
Curb weight	t	80
Gross weight	t	90
Reference vehicle for driving resistance		
Frontal area	m ²	10
Drag coefficient	–	0,75
Weight	t	82
Transmission ratio	–	5.5
Mass properties		
Moment of inertia	kg m ²	50
Wheel properties		
Friction coefficient of tire	–	0.7
Reference wheel load	kN	100
Wheel load correction coefficient	–	0.01
Rolling radius		
Static	mm	546
Dynamic	mm	550

Table 2. Technical data of fuel cell

Number of cell	–	4500
Cell area	cm ²	2720
CCL proton conductivity	A/(V cm)	3
Ideal open circuit voltage	V	1.23
Cat. layer thickness	cm	0.001
GDL thickness	cm	0.025
Maximum current	A	2500

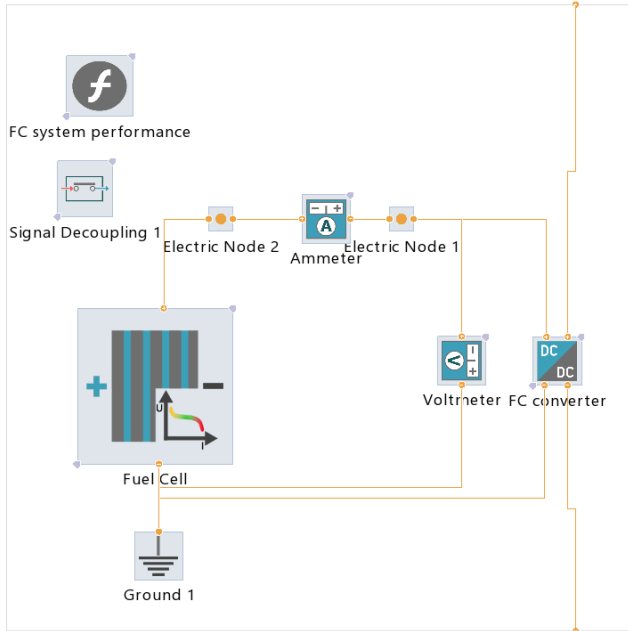


Fig. 3. Fuel cell model with measurement conditions and DC-DC voltage converter

The characteristics of the fuel cell stack used were shown in Fig. 4. The maximum power value was obtained with a current of about 1 kA. The cell voltage was limited to approximately 3.2 kV with these operating parameters. The operating temperature range of the cell stack was 30–80°C, at an air pressure of 1 bar and a humidity of 70%.

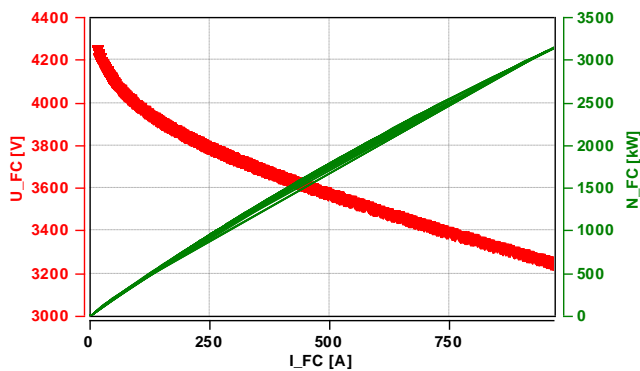


Fig. 4. Current-voltage characteristics of the fuel cell stack

5.2. Battery operating conditions

The locomotive system used two battery modules connected in series (Fig. 5). Each battery consisted of 4 rows of 262 cells connected in series. The cell volt-

age value was in the range of 3–5 V. The full specification of the battery cells was included in Table 3.

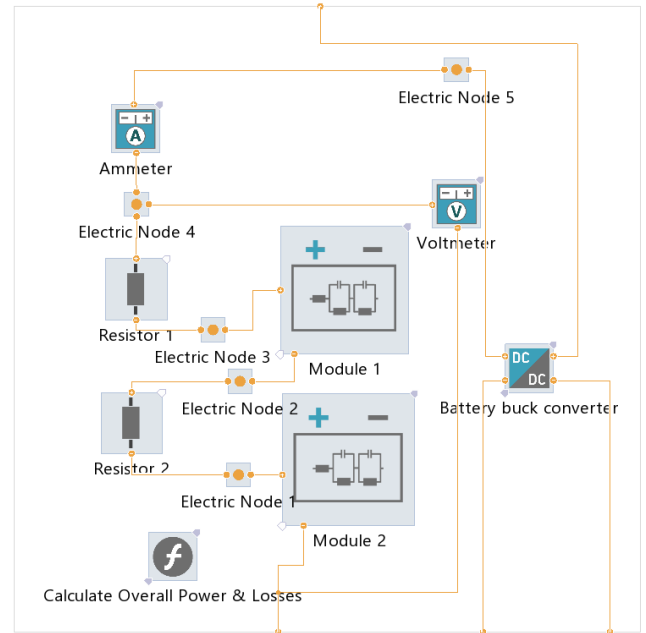


Fig. 5. Model of a high voltage batteries connected in series with a DC-DC voltage converter

Table 3. Technical data of battery

Number of cell per cell-row	–	262
Number of cell-rows	–	4
Minimum voltage	V	3
Maximum voltage	V	5
Maximum charge	Ah	25
Initial charge	%	60

The characteristics of a single battery cell were shown in Fig. 6. Assuming the battery state of charge (SOC) was in the range of 20–80%, the battery voltage was found to be in the range of 3.6–4.0 V.

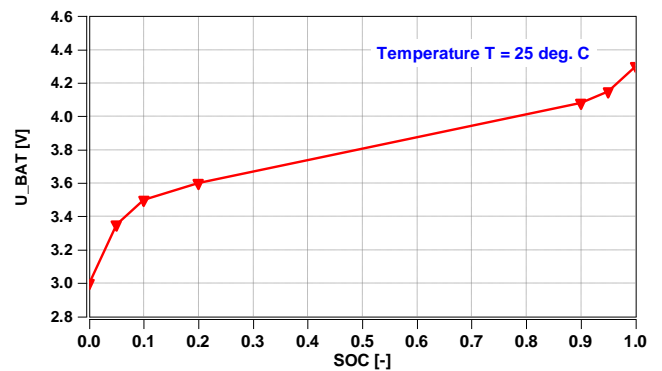


Fig. 6. Characteristics of the battery cell voltage depending on its charge level

The characteristics of resistance changes were shown in Fig. 7. It was assumed that these values dur-

ing the battery charging and discharging were the same.

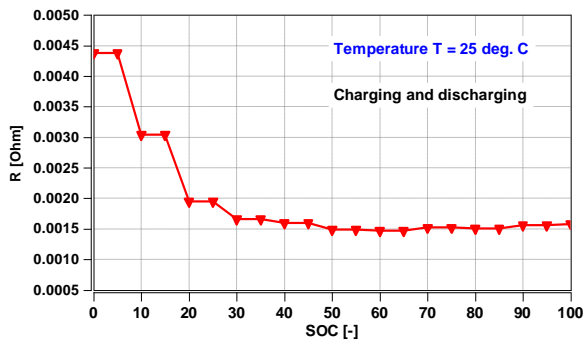


Fig. 7. Characteristics of the cell's resistance during charging and discharging

5.2. Electric motor operating conditions

The system used an asynchronous electric motor design operating in two quadrants (the first and the fourth). The torque characteristics were shown in Fig. 8. The maximum value of the torque was maintained up to the speed of 3000 rpm. The maximum engine speed was 7500 rpm. The engine was characterized by high efficiency values (over 90%) in the range of 2200–2500 rpm. When acting as a generator, however, the motor efficiency does not exceed 80%.

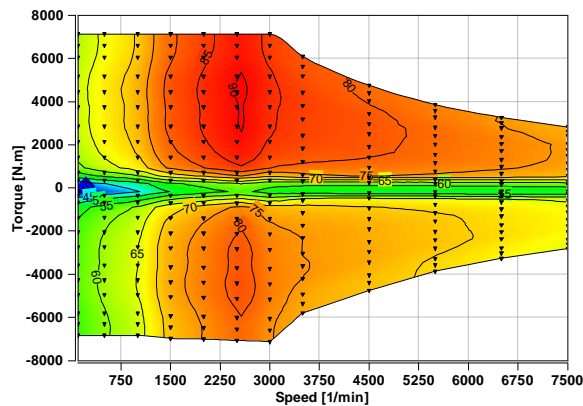


Fig. 8. Electric motor torque characteristics

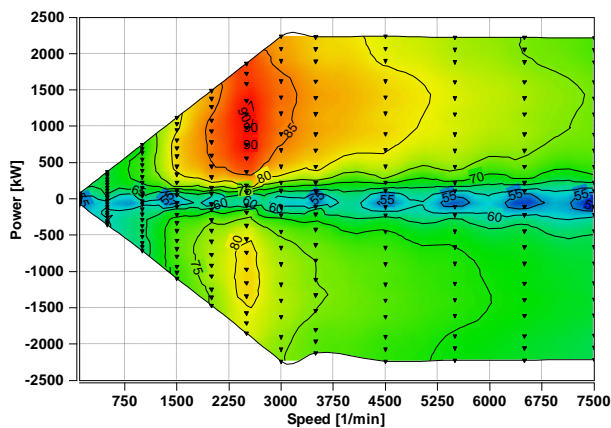


Fig. 9. Electric motor power characteristics

The electric motor power characteristic (Fig. 9) indicates constant power values in a fairly large range of rotational speeds. The maximum power of 2,240 kW can be obtained at a speed of 3,000 rpm.

5.3. Energy flow analysis

The route, simulated in the AVL Cruise M software, was used to analyze the energy flow. The 328 km route connects Helsingor in Denmark with Karlskrona in Sweden. The duration of the trip was 3 h 57 min. The maximum speed of the locomotive was 120 km/h. The driving speed profile of the locomotive was shown in Fig. 10.

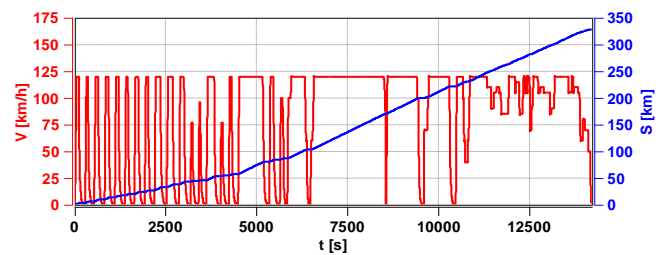


Fig. 10. Locomotive speed profile along with the distance covered

The data in Fig. 10 shows that the initial route was characterized by frequent stops. Longer sections of uniform drive speed can be found in the central part of the route. The final part of the route consisted of varying driving speeds, but without stopping the locomotive. As the profile shows, the first 30% of the route distance was covered more slowly, with frequent locomotive from stops. On the remaining 70% of the route the locomotive was travelling at a nearly constant speed. The mean travel speed was calculated to be about 83 km/h.

The values of the locomotive traction force and the power loss were also determined. These values were compiled into Fig. 11. The data shows that the average, maximum traction force was about 100 kN. The instantaneous, maximum power losses were measured at about 200 kW (the mean values results were determined by analyzing only the peaks of the values in Fig. 11).

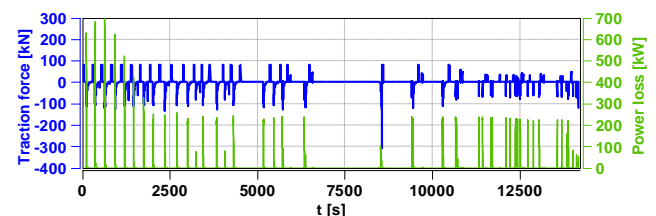


Fig. 11. Locomotive traction force and power loss

Because the fuel cell is the main source of the locomotive's propulsion, its power was more than twice that of the batteries. The operating conditions of the

fuel cell were shown in Fig. 12. The frequent change of the locomotive travel speed caused the cell current intensity to jump up to about 1000 A at certain points. As a result, the voltage drops to about 3200 V. Idle operation of the fuel cell (not providing power) caused the voltage to reach its maximum value. At steady speeds (approx. 120 km/h), the power drawn from the fuel cell was measured at 180 kW. The power drawn from the battery, however, was only 11 kW.

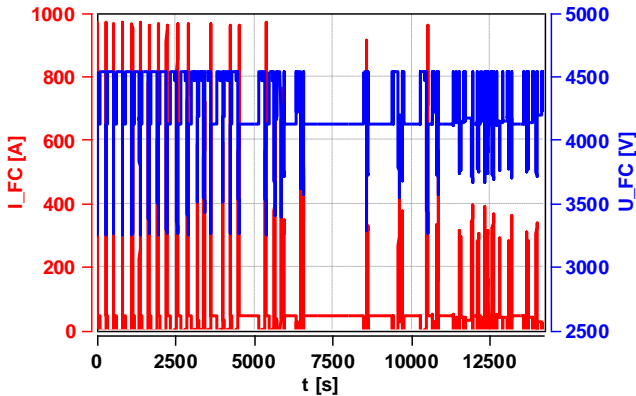


Fig. 12. Fuel cell operation characteristic when travelling on the simulated route

The drive system characteristics indicated that the maximum instantaneous power of the fuel cell stack reached 3 MW. About 1 MW of power was used in the final phase of the route, without stops but with a changes in travel speed. The total fuel cell energy value in the simulation was estimated at 0.875 MWh (Fig. 13).

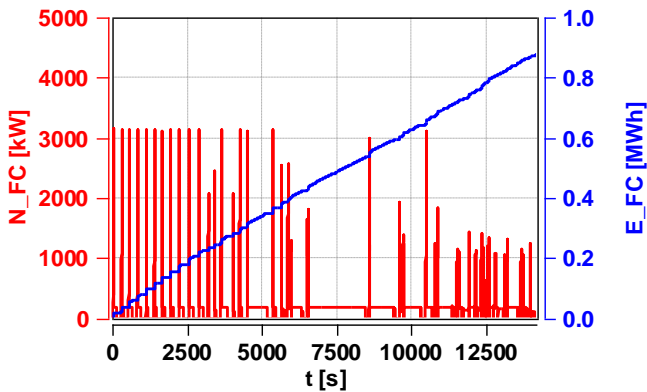


Fig. 13. The fuel cell power characteristics and its total energy consumption on the simulated route

A detailed analysis of a single acceleration (Fig. 14) after the locomotive stopped showed an almost two-fold decrease in the fuel cell voltage, with an increase in the current consumption to about 1000 A. This was mirrored by a slight decrease in the battery SOC. Subsequent locomotive braking caused this value to be greater (SOC = 0.61) than before braking

(SOC = 0.60). This means that when the locomotive brakes, it was possible to increase the SOC by 1%.

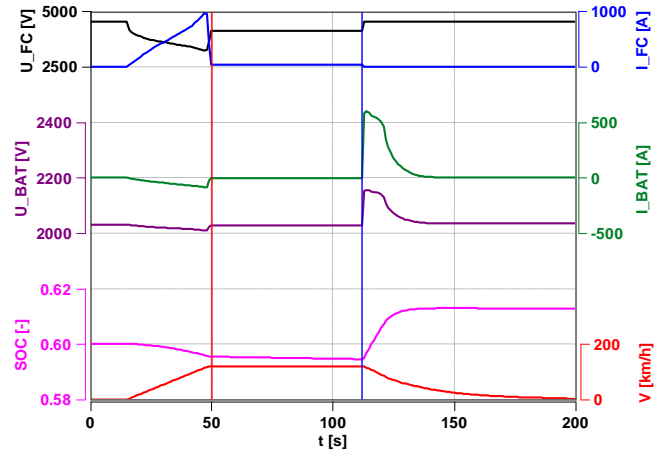


Fig. 14. Analysis of an individual speed profile change, including acceleration, constant speed and braking until the locomotive came to a stop

The voltage-current characteristic of the battery has shown much higher current values used during braking than during acceleration (Fig. 15). As the current value increased, the voltage value also increased. The density of test points increased at points of vehicle acceleration and braking. The characteristics in Fig. 15 show that the same current values (positive during braking and negative during acceleration) meant that the respective power values may be higher when the locomotive was braking. During braking, the voltages were found to be about 10% greater than the corresponding voltages during acceleration of the rail vehicle.

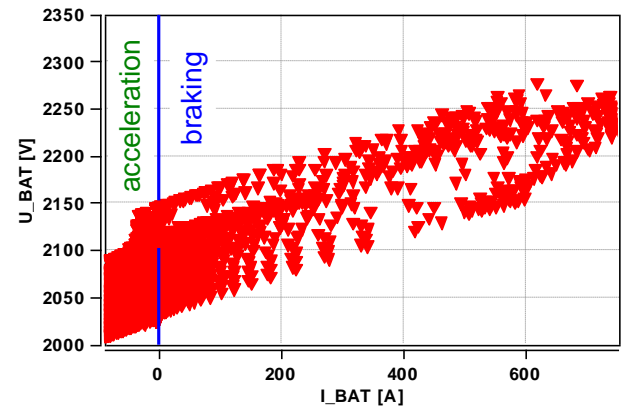


Fig. 15. Battery current-voltage characteristics

Analyzing Figs 14 and 15 indicated low values of the battery current used to drive the locomotive. Much higher currents (about 8 times) were used during braking of the vehicle. The highest currents occurred in the initial braking phase (Fig. 14) with the highest voltage values occurring at the same time. Under such condi-

tions, the maximum recovered power was approximately 1.7 MW.

The battery characteristics indicated its continuous recharging for the whole driving profile. This is due to an increase in the battery voltage (Fig. 16). The value of the current during the constant driving speed was about 200 A. Such values were obtained during the test time $t = 7500$ s. Each braking with the rail vehicle increased the charging current. The driving profile showed that the battery voltage increased by 110 V during the 320 km trip, which resulted in an increase in the battery charge level from 60% to over 90% (Fig. 17).

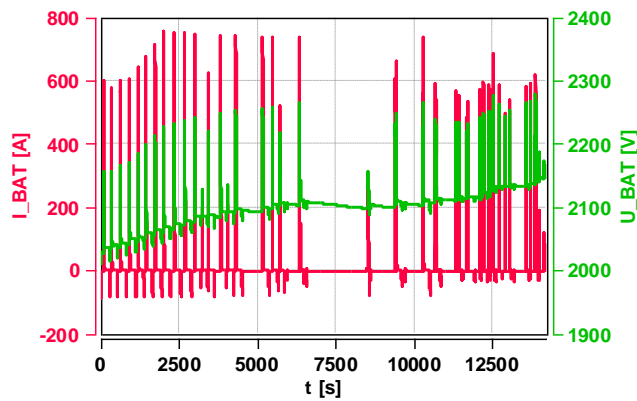


Fig. 16. Battery current-voltage characteristics for the simulated route

The maximum power drawn from the battery was about 1.8 MW (Fig. 17) when the locomotive was accelerating to a speed of 120 km/h. The value of the absolute increase in battery energy (including its discharge during acceleration) on the entire route was determined as 0.071 MWh (based on positive and negative current value from Fig. 16):

$$E_{\text{BAT}} = I_{\text{BAT}} \cdot U_{\text{BAT}} \cdot \Delta t \quad (2)$$

Almost 50% of this energy was obtained after travelling just the first 30% of the route distance. Thus proving that the hybrid drive solution used was very efficient.

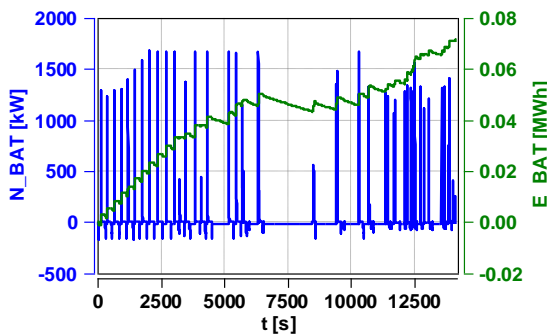


Fig. 17. Characteristics of battery power and total energy consumption throughout the simulated route

Although quite a large portion of the locomotive braking energy was recovered, the energy consumption of the fuel cell was nevertheless much higher and amounted to 0.875 MWh. The difference in energy consumption was therefore over 12 fold (Fig. 18).

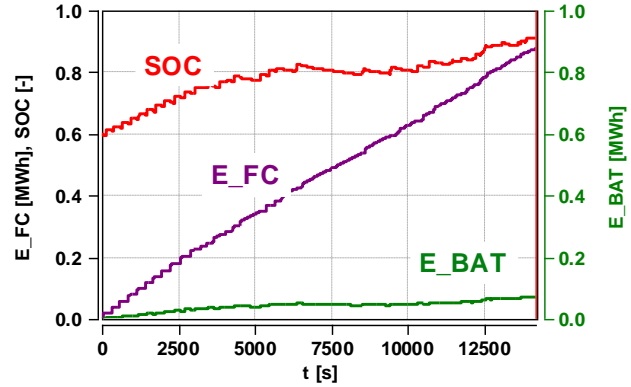


Fig. 18. Changes in energy consumption along with an increase in the battery charge level during the simulated journey

The hydrogen consumption during the fuel cell operation equaled 40.6 kg. Thus the average hydrogen consumption was 12.2 kg/100 km of the travel distance of a 82 t locomotive. Taking into account the energy used by the fuel cells and the energy recovered by the battery, then an average energy consumption value was of 245 kWh per 100 km of travel.

By taking into account the current values that were related to the battery power output, it is possible to determine the value of energy consumed by the battery.

The battery energy discharge value (only positive current value from Fig. 16 and eq. (2)) was 0.052 MWh.

This means that the energy recovery was 36% greater than the energy loss of the batteries for the locomotive drive ($0.071 \text{ MWh} / 0.052 \text{ MWh} \times 100\% = 36\%$).

6. Conclusions

The AVL Cruise M simulation environment is a software that enables a complete analysis of the energy flow in the drive system of a hybrid electric motor, fuel cells and batteries.

Based on the performed analyses, it has been concluded that:

1. The hybrid drive system (fuel cell, battery and electric motor) can be an alternative to electric or diesel drive systems of locomotives and passenger trains on passenger routes. Hydrogen storage and transportation remain an issue, however.

2. The 82 t locomotive can be powered by a 2.2 MW propulsion system without losing its drive properties up to a speed of 120 km/h.
3. The average energy consumption value of a locomotive weighing 82 t was 245 kWh/100 km; fuel cell hydrogen consumption was 12.2 kg/100 km.
4. Recuperative braking of the locomotive increased the absolute value of the battery SOC; this re-

mained true even after taking into account the battery power used to move the vehicle; the energy recovery for the batteries was 36% greater than the energy used to the locomotive drive.

Acknowledgements

This work has been done under AVL University Partnership Program.

Nomenclature

BAT	battery
CCL	cathode catalyst layer
DC	direct current
E	energy
EU	European Union
FC	fuel cell
GDL	gas diffusion layers
I	current
JR East	East Japan Railway Company
Li-Ion	Lithium-Ion battery

PEM	Proton Exchange Membrane
R	resistance
SC	supercondensator
SOC	state of charge
SOFC	solid oxide fuel cell
t	time
T	temperature
U	voltage
V	speed

Bibliography

- [1] Akhoundzadeh M.H., Panchal S., Samadani E. et al. Investigation and simulation of electric train utilizing hydrogen fuel cell and lithium-ion battery. *Sustainable Energy Technologies and Assessments*. 2021, **46**, 101234. <https://doi.org/10.1016/j.seta.2021.101234>.
- [2] Al-Hamed K.H.M., Dincer I. A new direct ammonia solid oxide fuel cell and gas turbine based integrated system for electric rail transportation, *eTransportation*. 2019, **2**, 100027, <https://doi.org/10.1016/j.etrans.2019.100027>
- [3] Al-Hamed K.H.M., Dincer I. A novel integrated solid-oxide fuel cell powering system for clean rail applications. *Energy Conversion and Management*. 2020, **205**, 112327. <https://doi.org/10.1016/j.enconman.2019.112327>
- [4] Coradia iLint. A full emission-free train. <http://aurichbahn.de/wordpress/wp-content/uploads/2012/07/Coradia-iLint-Product-sheet.pdf>
- [5] Coradia iLint™ – the world's 1st hydrogen powered train. <https://www.alstom.com/solutions/rolling-stock/coradia-ilinttm-worlds-1st-hydrogen-powered-train>
- [6] Deng K., Fang T., Feng H. et al. Hierarchical eco-driving and energy management control for hydrogen powered hybrid trains. *Energy Conversion and Management*. 2022, **264**, 115735. <https://doi.org/10.1016/j.enconman.2022.115735>.
- [7] D'Ovidio G., Ometto A., Valentini O. A novel predictive power flow control strategy for hydrogen city rail train. *International Journal of Hydrogen Energy*. 2020, **7**, 4922-4931. <https://doi.org/10.1016/j.ijhydene.2019.12.067>
- [8] Durzyński Z. Hydrogen-powered drives of the rail vehicles (part 1). *Rail Vehicles/Pojazdy Szynowe*. 2021, **2**, 29-40. <https://doi.org/10.53502/RAIL-139980>
- [9] Engineering ToolBox – Resources, Tools and Basic Information for Engineering and Design of Technical Applications! https://www.engineeringtoolbox.com/rolling-friction-resistance-d_1303.html
- [10] Eurostat. Road, rail and navigable inland waterways networks by NUTS 2 regions. <https://ec.europa.eu/>
- [11] Fragiaco P., Piraino F. Energy performance of a fuel cell hybrid system for rail vehicle propulsion. *Energy Procedia*. 2017, **126**, 1051-1058. <https://doi.org/10.1016/j.egypro.2017.08.312>
- [12] Fragiaco P., Piraino F. Fuel cell hybrid powertrains for use in Southern Italian railways. *International Journal of Hydrogen Energy*. 2019, **44**(51), 27930-27946. <https://doi.org/10.1016/j.ijhydene.2019.09.005>
- [13] Gechev T., Punov P. Popular fuel cell types - a brief review. *60th Annual Scientific Conference – University of Ruse and Union of Scientists*. Sofia. 2021, 57-66. <https://conf.uni-ruse.bg/bg/docs/cp21/4.1/4.1-13.pdf>
- [14] JR East, Hitachi and Toyota to develop hybrid (fuel cell) railway vehicles powered by hydrogen. 6.10.2020. <https://global.toyota/en/newsroom/corporate/33954855.html>
- [15] JR East, Hitachi and Toyota to develop hybrid fuel cell trains. *Fuel Cells Bulletin*. 2020, **11**, 6. [https://doi.org/10.1016/S1464-2859\(20\)30506-X](https://doi.org/10.1016/S1464-2859(20)30506-X)
- [16] Market Research Report. Hybrid Train Market by Propulsion Type (Electro Diesel, Battery Operated, Hydrogen, CNG, LNG, and Solar), Application (Passenger and Freight), Operating Speed (> 100 km/h,

- 100-200 km/h, < 200 km/h), Battery Technology, and Region – Global Forecast to 2030. August 2020. <https://www.marketsandmarkets.com/Market-Reports/hybrid-train-market-238438631.html>
- [17] Owano N. Bombardier electric hybrid train to keep Germany's green ambitions on track. <https://techxplore.com/news/2018-09-bombardier-electric-hybrid-germany-green.html>
- [18] Peng H., Chen Y., Chen Z. et al. Co-optimization of total running time, timetables, driving strategies and energy management strategies for fuel cell hybrid trains. *eTransportation*. 2021, **9**, 100130. <https://doi.org/10.1016/j.etrans.2021.100130>
- [19] Pielecha I., Engelmann D., Czerwinski J. et al. Use of hydrogen fuel in drive systems of rail vehicles. *Rail Vehicles/Pojazdy Szynowe*. 2022, **1**, 10-19. <https://doi.org/10.53502/RAIL-147725>
- [20] Ritter M. Hydrogen as the key for emission-free rail transport – opportunities and challenges. Alstom. 15.07.2017. <https://www.fch.europa.eu>
- [21] Sarma U., Ganguly S. Modelling and cost-benefit analysis of PEM fuel-cell-battery hybrid energy system for locomotive application. *2018 Technologies for Smart-City Energy Security and Power (ICSESP)*. 2018. <https://doi.org/10.1109/icsecp.2018.8376691>
- [22] Siemens. Mireo. <https://www.siemens.com/mireo>
- [23] Wachsman E.D., Lee K.T. Lowering the temperature of solid oxide fuel cells. *Science*. 2011, **334**(6058), 935-939. <https://doi.org/10.1126/science.1204090>